

Contribution of Self-Potential (SP) Measurements in the Study of Alpine Periglacial Landforms: Examples from the Southern Swiss Alps

Cristian Scapozza

Institute of Geography, University of Lausanne, Switzerland

Pierre Gex

Institute of Geophysics, University of Lausanne, Switzerland

Christophe Lambiel, Emmanuel Reynard

Institute of Geography, University of Lausanne, Switzerland

Abstract

Measurements of streaming potentials were carried out on rock glaciers and talus slopes in a test site of the southern Swiss Alps. After some theoretical considerations and a brief description of the measurement technique, a method of data treatment in high declivity topography is presented. The results of self-potential prospecting measurements are generally in accordance with the geomorphological observations. In particular, the groundwater runoff is influenced by the occurrence of permafrost, which creates surfaces of water migration partially independent from ground porosity.

Keywords: geophysics; rock glacier; self-potential; streaming potentials; Swiss Alps; talus slope.

Introduction

Self-potential (SP) (or spontaneous potential measurements) in the study of periglacial environments is a recent and not well-developed geophysical method in geomorphology, geocryology, and glaciology. Natural electrical potentials measurements have been carried out to monitor the thawing front movement and to study the active layer and permafrost parameters in arctic periglacial environments (e.g., Gahé et al. 1988, Fortier et al. 1993), for the study of subglacial drainage (e.g., Blake & Clarke 1999, Kulesa et al. 2003) or for the investigation of landslides (e.g., Bogoslawsky & Ogilvy 1977, Gex 1993).

In alpine periglacial environments, no studies on streaming potentials associated with groundwater runoff in rock glaciers and talus slopes have been carried out. Rock glacier hydrology has been studied with water tracing (e.g., Tenthorey 1992, Krainer & Mostler 2002) or thanks to borehole logging (e.g., Haeberli 1985, Vonder Mühl 1992), whereas talus slope hydrology is not well known (e.g., Rist & Phillips 2005).

The present paper presents and discusses results of streaming potentials mapping in the Sceru Valley (Fig. 1), in the Eastern part of the Blenio Valley (Lepontine Alps of the Tessin, southern Switzerland). The objectives are to present the measurement technique and a method of data treatment in high declivity topography.

Theory and Methods

Macroscopic streaming potential mapping was realized from field measurements carried out in 2006 and 2007. The method is completed by geomorphological observations and mapping, frequency-domain electromagnetic lateral mapping and 2D resistivity profiling (Geonics EM-16R and EM-31), direct current (DC) resistivity soundings, and

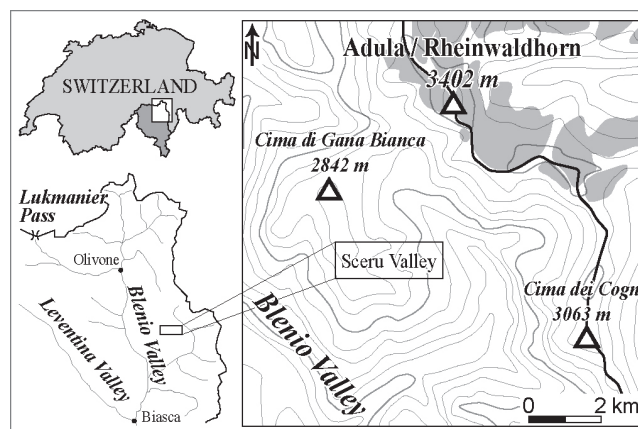


Figure 1. Geographical location of the study area.

thermal prospecting (miniature ground temperature data loggers and spring temperatures). In this paper, only the field measurement technique and the interpretation of large geomorphological structures ($> 1000 \text{ m}^2$) are presented.

The streaming potentials

Streaming potentials, or electrofiltration potentials, are natural electrical potentials produced by water flow through a porous and permeable soil (Reynolds 1997). The streaming potentials are directly proportional to the selective filtration of ions (electrofiltration) at the microscopic scale. Water, acting as an electrolyte, creates at the interface mineral-water a positive load flow between the immobile part of the electrical double layer (composed by the Stern layer—in contact with the mineral and with fixed cations, and the Gouy-Chapman diffuse layer—with a lower cations concentration) and the free neutral electrolyte (Revil et al. 2004). The Helmholtz-Smoluchowski law links up the electrofiltration potential (EF) amplitude with the electrolyte characteristics:

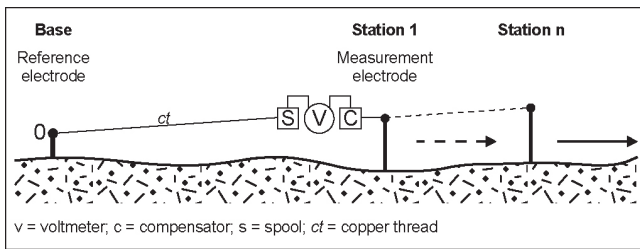


Figure 2. Field acquisition of self-potential data.

$$EF = \frac{\rho \varepsilon \zeta}{4 \pi \eta} \Delta P \quad (1)$$

where ρ is the resistivity, ε the dielectric constant and η the dynamic viscosity of the electrolyte. ζ is the electrical potential of the double layer (zeta potential) and ΔP is the pressure difference between the measurement points of EF.

Ultra-fresh and fresh groundwaters induce the maximum electrofiltration fields (Bogoslowsky & Ogilvy 1973). Indeed, in presence of much conductive water (with a mineral concentration exceeding 5 g/l), the electrolyte short-circuits the spontaneous electrical current.

Self-potential variations are also due to the granulometry and permeability of the soil. In a homogenous and isotropic terrain and where granulometry and permeability are known, the streaming potentials reflect the contours of the water table. In this case, self-potential mapping and inversion can supply information about some characteristics (configuration, direction, and intensity) of seepage flow both in horizontal and vertical planes (Revil et al. 2004).

Measurement of streaming potentials

SP is a passive method. The technique applied in this study is based on the fact that each value of self-potential measured at the ground surface is linked up with one electrode fixed at a base station situated outside of the geomorphological landforms studied. The potential difference (in mV) is measured between the reference electrode and a measurement electrode, which is moved along a traverse (Gex 1993, Reynolds 1997).

The range of the measured potentials is generally comprised between several millivolts (mV) and one volt. Because the sign of the zeta potentials could be positive or negative according to the earth materials, the sign of the difference of voltage measured is an important factor for the interpretation of SP anomalies (Reynolds 1997). For convention, the self-potential value at the reference electrode is zero. SP cartography has been carried out with a distance between every measurement of 3 to 5 m.

The measurement material used in this study was developed at the Institute of Geophysics of the University of Lausanne. The reference electrode of the model non-polarisable with Cu-CuSO_4 was realized in PVC and wood. The measurement electrode is fixed on a stick one meter long; its thin section allows us to drive it into the ground comfortably. It is linked up with the reference electrode by an isolated copper wire. A spool, fixed on the back of the operator, permits us to unwind the copper wire. The measurements are carried out with a

high impedance (100 M Ω) digital voltmeter. The scale range of the voltmeter is comprised between -2000 and 2000 mV. A compensator is associated with the voltmeter to settle the SP value to the zero at the reference electrode. Finally, the voltmeter is provided with a filter that permits us to stabilize the measurements when the ground presents perturbations to the natural electrical fields. The field data acquisition is schematized in Figure 2.

Very Low Frequency-Resistivity (VLF-R)

The VLF-R technique (see Hoekstra et al. 1975, Hoekstra 1978, McGrath & Henderson 1985) uses electromagnetic energy radiated by a very low frequency (VLF) transmitter. In this study the Hauderfehn transmitter (23.4 kHz) located in Germany was used. The measurement of the horizontal component of the electric field and of the horizontal magnetic component perpendicular to the azimuth of the transmitting station allows the apparent resistivity of the near surface to be determined using the Cagniard (1953) equation:

$$\rho_a = (0.2/f)(E/H)^2 \quad (2)$$

where ρ_a is the apparent resistivity (Ωm), f the frequency (Hz), E the electric field (mV/km) and H the magnetic field (nT). The ratio between H and E gives a phase angle that changes according to variations of resistivity with the depth.

The field data acquisition was carried out using a Geonics EM-16R instrument.

Field Site Characteristics and Data Acquisition

The Sceru Valley (46°27'N, 9°01'E) is an east-facing glacial cirque situated between 2000–2787 m a.s.l. The morphology and hydrology of the Sceru Valley were studied by Scapozza (2008). The morphology is characterized by the presence of several rock glaciers with different degree of activity, talus slopes, and Lateglacial moraines (Fig. 3).

Permafrost is present in the Piancabella rock glacier and in the lower part of the Gana Rossa talus slope (Scapozza 2008). The hydrology of the southern part of the Sceru Valley is influenced by the presence of rock glaciers. Because of the high porosity of the blocky surface, no subaerial water runoff can be observed (the spring in the lower part of the Gana Rossa talus slope is situated one meter below the ground surface).

In 2006 and 2007, 17 SP profiles were carried out on the Sceru I rock glacier, 2 on the Piancabella rock glacier, 1 on the Gana Rossa talus slope, and 2 on the Sasso di Luzzone talus slope/rock glacier complex. In total, about 1300 SP measurement points were listed.

In the talus slopes and the active rock glacier, several SP profiles were combined with Geonics EM-16R and/or EM-31 mapping along the same traverse.

Results and Discussion

Data treatment

In high declivity topography like the alpine periglacial

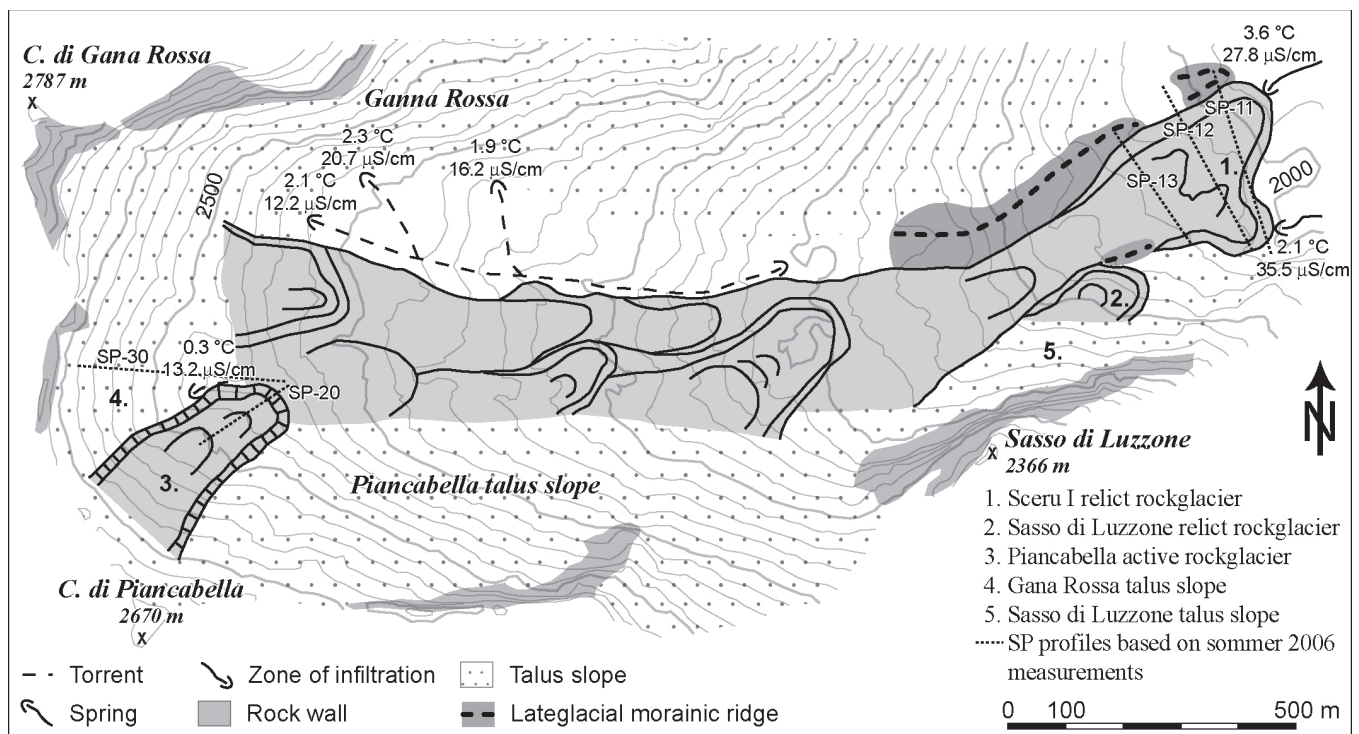


Figure 3. Geomorphological map of the Sceru Valley. For further information, see Scapoza (2008).

environment, the natural streaming potential linked to the slope is important, and its effect on the difference of voltage (in mV) measured by self-potential prospecting is very high. This perturbation, named “Topographic Effect” (TE), has been known to geophysicists for more than 90 years (Ernstson & Scherer 1986). The TE presents, for a constant electric field, an increasing negative potential linked with the elevation in altitude. For these reasons the regional anomaly (due to the TE) has to be subtracted from the measured values, which gives a final residual anomaly. The TE is calculated with a statistical analysis of linear regression between self-potential data and altitude. In practice, the average of the first four values of 11 traverses, measured between 2000–2450 m outside of the body of the Sceru I rock glacier, were used to calculate the TE, with a correlation between SP and altitude of -0.86 . The calculated gradient of the TE is -68 mV per 100 m difference in elevation.

SP data were exposed in the form of potential profiles and equipotential maps. For the equipotential maps, a geostatistical interpolation of SP data was made with ordinary kriging. All the SP data (except for profiles SP-20 and SP-30) refer to the reference electrode placed outside the Sceru Valley (Fig. 4). For profiles SP-20 and SP-30, the reference electrode was placed at the Swiss Grid coordinates $720^{\circ}215/145^{\circ}660$, at 2460 m a.s.l.

Sceru I relict rock glacier

The SP prospecting of this rock glacier shows an almost continuous negative residual anomaly in the northern lobe and another negative residual anomaly in the southern lobe. A zero millivolt residual anomaly is located between the Sceru I rock glacier and the Sasso di Luzzone talus slope/

rock glacier complex situated south of it (Fig. 4).

According to the geoelectrical prospecting (2 DC resistivity soundings and one 2D resistivity profile), the bulk resistivity structure of the rock glacier seems to be relatively homogeneous. Indeed, the ground apparent resistivity is comprised between 3–5 $k\Omega m$ (Scapoza 2008).

The groundwater runoff of two springs with different temperatures and electrical conductivities situated at two different lobes of the rock glacier could be followed by the self-potential prospecting (Figs. 4, 5). The link between the negative anomaly and the groundwater runoff is clearly evidenced in three SP profiles executed in summer 2006 (Fig. 5).

The two continuous anomalies may indicate the presence of two locations of preferential saturated groundwater flow. The two systems are probably independent, as evidenced from the constant difference throughout the year of temperature and conductivity of the two springs situated at the front of the rock glacier. Following this hypothesis, SP measurements would confirm that the two springs are alimented with groundwater of different origin (Fig. 4).

The torrents situated in the northern part of the Sceru Valley possibly feed the northern lobe spring (as pointed out by a warming of water temperatures), whereas the southern lobe spring would be alimented by an important aquifer situated into the Sceru I rock glacier. This water may be stored in the rock glacier for several months. The relatively high water conductivity (compared to the other springs in the valley, see Figure 3) and the constant water temperature (between $2.0^{\circ}C$ and $2.2^{\circ}C$) all year long would confirm that the water transfer in this rock glacier is very slow, as it was pointed out by Tenthorey (1992) in a similar environment.

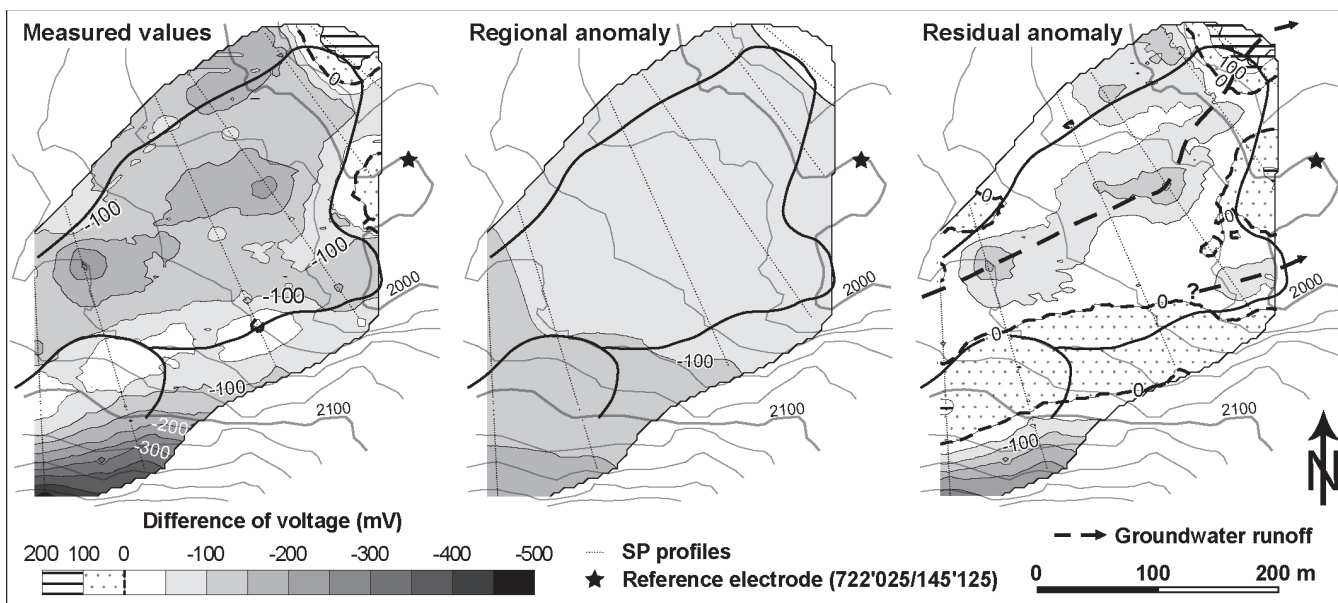


Figure 4. SP equipotential map of the Sceru I rock glacier and the Sasso di Luzzzone talus slope/rock glacier complex based on summer 2007 measurements. For topographic names, see Figure 3.

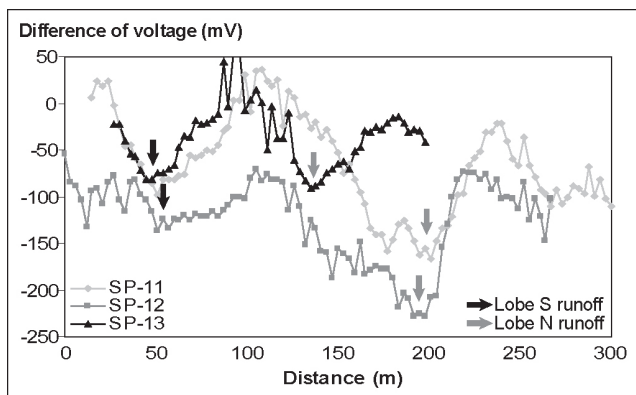


Figure 5. SP profiles executed across the Sceru I rock glacier. The arrows show negative anomalies linked with groundwater runoff. For the location of SP profiles, see the Figure 3.

The cold water temperature of the southern spring may be linked to a process of winter-ascending air circulation (the so-called chimney effect), which facilitates the cooling of the ground in the lower part of a porous sediment deposit (Delaloye & Lambiel 2005).

Piancabella active rock glacier

Prospecting of this landform shows a rise of the SP at the foot of the rock glacier front and a low increase of SP values all along the rock glacier (Fig. 6). Because of the location of the reference electrode (settled to 0) downslope of the rock glacier, the rise of the SP at the front can be interpreted as an important negative residual anomaly of several hundred mV.

A VLF-R tomography performed with the 2LayInv software (Pirttijärvi 2006) allows us to know approximately the active layer depth and the permafrost resistivity. The parameters of the profiling inversion are presented in Figure 6. Maximal VLF-R resistivities are found at the front of the rock glacier, and a decrease of the values toward upslope

can be observed. Between 30–70 m, the decrease in the resistivities coincides with a decrease of the active layer depth. At 75 m, an important groundwater runoff has been perceived beneath the surface.

Data from the Piancabella active rock glacier show a connection between changes in SP, changes in active layer properties (particularly, its depth), changes in permafrost structure and/or in bulk resistivity structure (as shown by the VLF-R tomography). Indeed, the correlation between SP and active-layer depth is -0.74, whereas it is -0.85 between SP and permafrost resistivity. The correlation between SP and altitude (in m) is 0.54, which confirms that SP is partially independent from topography.

The permafrost resistivity depends on ground temperature, permafrost ice resistivity and content, and unfrozen water resistivity and content (Haerberli & Vonder Mühl 1996). Thus, it is difficult to separate the effect of change in water conductivity on SP from those on bulk resistivity.

The good connection between SP and permafrost resistivity probably indicates that there is a constant and continuous groundwater flow of constant water electrical conductivity and constant temperature throughout the active layer, and that SP changes are due to changes in the bulk resistivity structure of the rock glacier. This would confirm that the suprapermafrost groundwater runoff is supplied by the melt of annual névés at the root of the rock glacier and by the addition of incidental rainfall (see Tenthorey 1992). It is difficult to know the proportion of ice melt in the active layer and/or at the permafrost table, which is probable for a rock glacier situated at the lower limit of discontinuous permafrost.

Finally, the negative SP residual anomaly at the foot of the rock glacier front evidences an important groundwater runoff. This groundwater runoff is probably linked to suprapermafrost and intra- and subpermafrost water flow, which concentrates at the foot of the rock glacier front (Haerberli 1985).

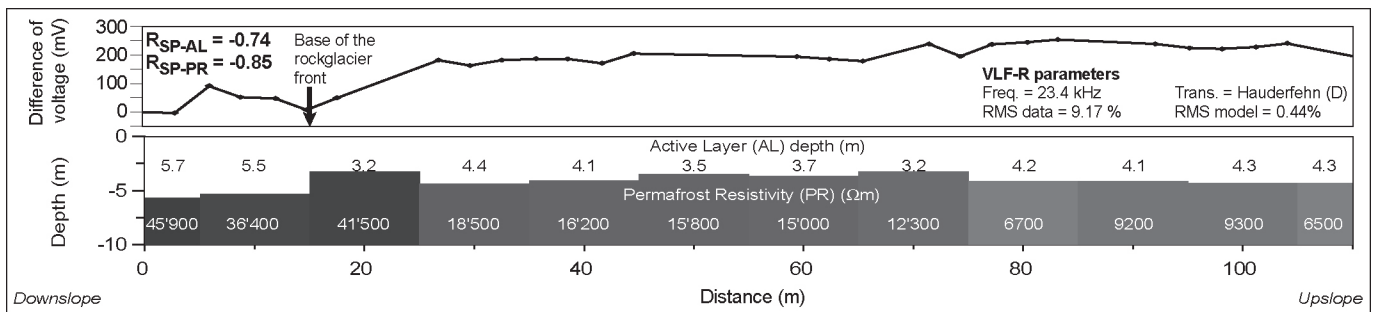


Figure 6. Profile SP-20 (at the top) and VLF-R tomography (below) on the Piancabella rock glacier. The VLF-R profiling inversion was performed with the 2LayInv (©University of Oulu) software (Pirttijärvi 2006).

Gana Rossa talus slope

SP prospecting of the Gana Rossa talus slope (Fig. 7) shows two negative residual anomalies in the lower part of the landform and an important and well-developed positive anomaly between 60–160 m distance. Another positive anomaly is present in the upper part of the talus slope. VLF-R prospecting shows relatively high apparent resistivities (over that 10,000 Ωm) in the lower part and in the middle of the talus slope. According to DC-resistivity, EM-31 and thermal prospecting (Scapozza 2008), permafrost is present only in the lower part of this talus slope (Fig. 7).

The streaming potentials are weakly positively correlated with altitude ($R = 0.54$), which contrasts with the theory of the TE (see *Data treatment*). Indeed, a test made in the Sasso di Luzzone talus slope (Fig. 3), where permafrost is absent, gives a very high negative correlation between streaming potentials and altitude ($R = -0.97$). Some results were pointed out by other studies carried out in high declivity slopes (e.g., Jackson & Kauahikana 1988).

Comparison between SP measurements and permafrost distribution shows, for the lower part of the talus slope, a connection between SP residual anomalies and permafrost occurrence. A possible hypothesis to explain this SP positive residual anomaly is the following: the presence of saturated or partially under-saturated permafrost may create a relatively impermeable surface of water runoff, which may modify the direction of the natural streaming potential linked to the slope (which is present between 120–200 m, as pointed out by the negative correlation between streaming potentials and altitude) by the canalization of groundwater flow at the base of the active layer. Following this hypothesis, the negative SP residual anomaly situated at a distance of 25 m may be related to an important water infiltration in the porous sediments, supplied by the melt of annual névés and by the addition of incidental rainfall. Whereas, the negative SP residual anomaly situated at a distance of 50 m may be related to the presence of a talik that would permit an intrapermafrost groundwater flow. The important groundwater runoff in the lower part of the talus is also proved by a spring (Fig. 3). Finally, in the upper part of the talus slope, the SP variations are probably due to the topography of bedrock, which is located only a few meters below the slope surface.

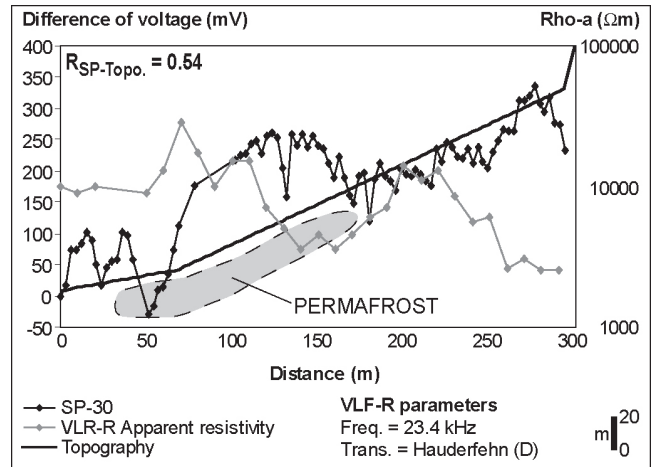


Figure 7. SP profile across the Gana Rossa talus slope.

In conclusion, it is very difficult today to better detail the hydrological and glaciological behavior of this talus slope without short, medium, and long-term thermal and geophysics monitoring at the surface and in boreholes.

Conclusions and Perspectives

The examples discussed show that measurement of streaming potential change on periglacial landforms offers good possibilities for assessing changes in water content and migration. Self-potential measurement could be useful for studying, in accordance with other geophysical methods, the importance of groundwater runoff generated by water infiltration and/or ice melting in permafrost terrains. The repetition of the same SP profile ten months later on a relict and an active rock glacier gave the same results; this confirms that streaming potential monitoring in periglacial landforms is possible. Self-potential monitoring associated with thermal and Electrical Resistivity Tomography (ERT) monitoring could be interesting for quantifying the processes correlated with permafrost degradation in high mountain environments.

Acknowledgments

Special thanks are due to all people who helped in the field, to the Associate Editor and the two anonymous reviewers for their useful feedback, and to Meredith Blake for proofreading the English.

References

- Blake, E.W. & Clarke, G.K. 1999. Subglacial electrical phenomena. *Journal of Geophysical Research* 104 (B4): 7481-7495.
- Bogoslowky, V.V. & Ogilvy, A.A. 1973. Deformations of natural electric fields near drainage structures. *Geophysical Prospecting* 21: 716-723.
- Bogoslowky, V.V. & Ogilvy, A.A. 1977. Geophysical methods for the investigation of landslides. *Geophysics* 42: 562-571.
- Cagniard, L. 1953. Basic theory of the magneto-telluric method of geophysical prospecting. *Geophysics* 18: 605-635.
- Delaloye, R. & Lambiel, C. 2005. Evidence of winter ascending air circulation throughout talus slopes and rock glaciers situated in the lower belt of alpine discontinuous permafrost (Swiss Alps). *Norsk Geografisk Tidsskrift* 59: 194-203.
- Ernstson, K. & Scherer, H.U. 1986. Self-potential variations with time and their relation to hydrogeologic and meteorological parameters. *Geophysics* 51: 1967-1977.
- Fortier, R., Allard, M. & Seguin, M.-K. 1993. Monitoring thawing front movement by self-potential measurements. *Proceedings of the Sixth International Conference on Permafrost, Beijing, China, July 5-9, 1993*: 182-187.
- Gahé, E., Allard, M., Seguin, M.-K. & Fortier, R. 1988. Measurements of active layer and permafrost parameters with electrical resistivity, self potential and induced polarisation. *Proceedings of the Fifth International Conference on Permafrost, Trondheim, Norway, 2-5 August, 1988*: 148-153.
- Gex, P. 1993. Mesures d'électrofiltration sur le glissement de la Frasse (Préalpes romandes). *Hydrogéologie BRGM* 3: 239-246.
- Haerberli, W. 1985. Creep of mountain permafrost: internal structure and flow of alpine rock glaciers. *Mitteilungen der VAW/ETH Zürich*: 77.
- Haerberli, W. & Vonder Mühll, D. 1996. On the characteristics and possible origin of ice in rock glacier permafrost. *Zeitschrift für Geomorphologie N. F., Suppl.-Bd.* 104: 43-57.
- Hoekstra, P. 1978. Electromagnetic methods for mapping shallow permafrost. *Geophysics* 43: 782-787.
- Hoekstra, P., Sellmann, P.V. & Delaney, A. 1975. Ground and airborne resistivity surveys of permafrost near Fairbanks, Alaska. *Geophysics* 40: 641-656.
- Jackson, D.B. & Kauahikana J. 1988. Regional self-potential anomalies at Kilauea volcano. *Prof. Pap. U.S. Geological Survey* 1350: 947-959.
- Krainer, K. & Mostler W. 2002. Hydrology of active rock glaciers: examples from the Austrian Alps. *Arctic, Antarctic, and Alpine Research* 34: 141-149.
- Kulesa, B., Hubbard, B. & Brown, G.H. 2003. Cross-coupled flow modeling of coincident streaming and electrochemical potentials and applications to subglacial self-potential data. *Journal of Geophysical Research* 108 (B8): 2381, DOI:10.1029/2001JB001167.
- McGrath, P.H. & Henderson, J.B. 1985. *Reconnaissance Ground Magnetic and VLF Profile Data in the Vicinity of the Thelon Front, Artillery Lake Map area, District of Mackenzie*. Paper-Geological Survey of Canada 85-1A: 455-462.
- Pirttijärvi, M. 2006. *2LAYINV – Laterally Constrained Two-layer Inversion of VLF-R Measurements*. User's guide, Division of Geophysics, University of Oulu.
- Revil, A., Naudet V., Meunier, J.D. 2004. The hydroelectrical problem of porous rocks: inversion of the position of the water table from self-potential data. *Geophysical J. International* 159: 435-444.
- Reynolds, J.M. 1997. *An Introduction to Applied and Environmental Geophysics*. Chichester: Wiley, 796 pp.
- Rist, A. & Phillips, M. 2005. First results of investigations on hydrothermal processes within the active layer above alpine permafrost in steep terrain. *Norsk Geografisk Tidsskrift* 59 : 157-163.
- Scapozza, C. 2008. *Contribution à l'étude géomorphologique et géophysique des environnements périglaciaires des Alpes Tessinoises orientales*. M.S. Thesis. Institute of Geography, University of Lausanne. Published February 28, 2008, on <http://doc.rero.ch/>
- Tenthorey, G. 1992. Perennial nevés and the hydrology of rock glaciers. *Permafrost and Periglacial Processes* 3: 247-252.
- Vonder Mühll, D. 1992. Evidence of intrapermafrost groundwater flow beneath an active rock glacier in the Swiss Alps. *Permafrost and Periglacial Processes* 3: 169-173.